Bio-inspired synthesis of crystalline TiO 2 : Effect of amino acids on nanoparticles structure and shape

Joachim Bill, Fritz Aldinger, Olivier Durupthy

Bio-inspired synthesis of crystalline TiO_2: Effect of amino acids on nanoparticles structure and shape.

Olivier Durupthy*, Joachim Bill, and Fritz Aldinger

Max-Planck-Institut für Metallforschung and Institut für Nichtmetallische Anorganische

Materialien, Universität Stuttgart, Pulvermetallurgisches Laboratorium, Heisenbergstrasse 3,

D-70569 Stuttgart, Germany

Crystalline titanium dioxide particles were obtained through the thermo-hydrolysis at 60°C of aqueous $TiCl_4$ precursor in the presence of various amino acids. These protein building blocks were employed to modify the phase distribution, size and shape of the formed nanoparticles. The consequences of the presence of biological species during the different steps of the inorganic condensation were characterized by a variety of techniques, including X-Ray diffraction, transmission electron microscopy and thermogravimetric analysis coupled with differential scanning calorimetry. The amino acids side chain functions were shown to be of a particular importance in regard to the modification of the TiO_2 structure and morphology. More specifically, aspartic acid, glutamic acid and serine allowed the formation of pure anatase nanoparticles. The pH of the reacting solution was also proved to be a relevant parameter to control the particle size and shape (cf micrograph, scale bar 5nm). Explanations based on the actual knowledge on the titania-amino acids interface were proposed for every observed modification.

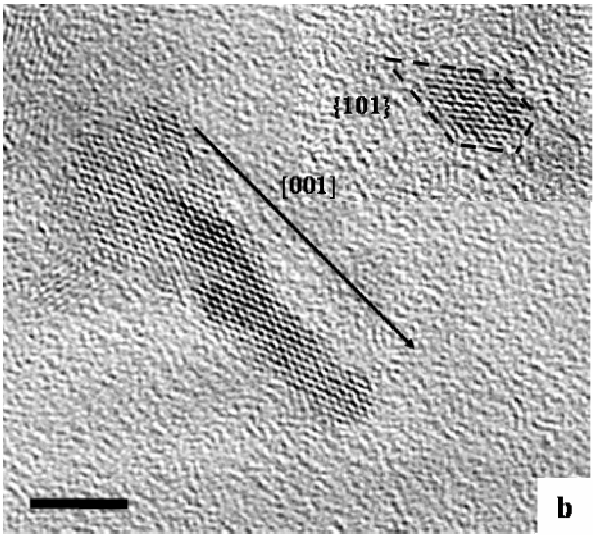

Dr. Olivier Durupthy

Max-Planck-Institut für Metallforschung

Heisenbergstrasse 3

D-70569 Stuttgart, Germany

Tel/Fax: +49(0)711 689 3226/3131

durupthy@ccr.jussieu.fr

Bio-inspired synthesis of crystalline TiO_2: Effect of amino acids on nanoparticles structure and shape.

Olivier Durupthy, Joachim Bill, and Fritz Aldinger*

Max-Planck-Institut für Metallforschung and Institut für Nichtmetallische Anorganische Materialien, Universität Stuttgart, Pulvermetallurgisches Laboratorium, Heisenbergstrasse 3, D-70569 Stuttgart, Germany

* durupthy@ccr.jussieu.fr

RECEIVED DATE (to be automatically inserted after your manuscript is accepted if required according to the journal that you are submitting your paper to)

CORRESPONDING AUTHOR FOOTNOTE

Telephone number +49(0)711 689 3226, fax number: +49(0)711 689 3131, and e-mail address durupthy@ccr.jussieu.fr.

Crystalline titanium dioxide particles were obtained through the thermo-hydrolysis at 60°C of aqueous $TiCl_4$ precursor in the presence of various amino acids. These protein building blocks were employed to modify the phase distribution, size and shape of the formed nanoparticles. The consequences of the

presence of biological species during the different steps of the inorganic condensation were characterized by a variety of techniques, including X-Ray diffraction, transmission electron microscopy and thermogravimetric analysis coupled with differential scanning calorimetry. The amino acids side chain functions were shown to be of a particular importance in regard to the modification of the TiO_2 structure and morphology. More specifically, aspartic acid, glutamic acid and serine allowed the formation of pure anatase nanoparticles. The pH of the reacting solution was also proved to be a relevant parameter to control the particle size and shape. Explanations based on the actual knowledge on the titania-amino acids interface were proposed for every observed modification.

Introduction

Research on titania powder synthesis is motivated by its numerous applications such as pigment,[1] UV blocker,[2] photocatalyst,[3-5] electrochromic material,[6, 7] oxygen sensor,[8, 9] lithium-ion battery[10] and dye-sensitized solar cell (DSSC).[11] The efficiency of the oxide in each of those applications depends on the phase, size and shape of the particles used. Indeed, it is well-known that the anatase polymorph displays a higher photoactivity than brookite or rutile.[12] However, a pure polymorph is not always easy to obtain and mixtures of various polymorphs are often observed in commercially available photocatalysts: Degussa P-25 contains a maximum anatase amount of 80%. Rutile, the thermodynamically stable polymorph,[13] is obtained by high temperature synthesis but with a lower control over particle size and shape. In order to obtain the metastable polymorphs anatase and brookite, or to form rutile crystals in the nanometer size range with a controlled shape, sol-gel methods were developed. These methods are mainly hydrothermal synthesis[14-16] and hydrolysis and condensation of alkoxides or aqueous Ti(IV) precursors.[17-19] In these more gentle conditions, the use of mineral[20] or organic[21-26] additive as well as specific acidic or alkaline conditions[27, 28] allowed to tailor precisely both titania structure and morphology.

In the field of the controlled synthesis of inorganic materials, living organisms were proved to be very efficient even in aqueous solutions and at ambient temperatures. Shells and sea urchins can synthesize a mineral defense made of calcium carbonate with a defined structure and a morphological control from the nanometer to the centimeter scale.[29] Nanometric magnetic iron oxide particles were also found in magnetotactic bacteria.[30] In every case, proteins and biological membranes are involved in the biomineralization process. The geometry, charge and chemical functions at the surface of those proteins are of particular importance in the control of the inorganic condensation.[31, 32]

The work presented here aims at synthetic methods for titanium oxide nanoparticles in which biomolecules are used to tune the structure and the morphology of the final material. Amino acids, the proteins building units, represent an interesting first step in this bio-inspired approach as they display a variety of chemical functions. They can consequently interact with the Ti(IV) precursors in solution or with the different titania surfaces. In this study, amino acids were introduced in a $TiCl_4$ aqueous solution and precipitation and crystallization of titania studied by adjusting the pH of the solution and by thermo-hydrolysis at 60°C. The influence of various synthesis parameters such as the solution pH, the nature and amount of the introduced amino acid was studied, thus allowing a discussion of possible bio-inorganic interactions.

Experimental section

Synthesis. A stock solution with a Ti^{4+} ion concentration of 0.5 $mol.L^{-1}$ was prepared by slow dilution of $TiCl_4$ (Fluka) in cooled HCl (3 $mol.L^{-1}$) solution. 4.0 mL of the stock solution were introduced in 46.0 mL of Milli-Q water at room temperature. A defined amount of selected amino acid was then introduced as powder under a vigorous stirring. The chemical structures and acidic properties of the used amino acids are given in Table 1. No precipitation occurred during the mixing. The pH of the mixture was adjusted to a selected value by addition of NaOH (2.0, 1.0 and 0.1 $mol.L^{-1}$ solutions) and the sample volume was completed to 100.0 mL with Milli-Q water. The concentration of Ti^{4+} and amino

acids became 20 mmol.L^{-1} and 1 to 80 mmol.L^{-1} (40 mmol.L^{-1} when not mentioned) respectively. A white precipitate appeared immediately with alkalinisation. The pH of the sample was controlled again after few minutes of stirring and readjusted to the set value. Several samples were prepared in the $1 \leq pH \leq 8$ range. Suspensions were aged for periods comprise between one day and one week in a stove at 60 °C without stirring. Solids were collected by centrifugation of the colloidal suspensions and the pH of the remaining supernatant solutions was recorded. Precipitates were washed, ultrasonicated and centrifuged twice with water whose pH was set to the one of the synthesis with few drops of hydrochloric acid. Finally, powders were dried under argon flow at room temperature.

Methods. Titanium concentration in solution was determined by spectroscopic measurement, on a Varian Cary 5000 spectrometer, of the stable orange complex, $[Ti(O_2)(OH)(H_2O)]^+$, formed by the addition of H_2O_2 to an acidic Ti^{4+} solution ($2.10^{-4} \leq [Ti^{4+}] \leq 2.10^{-3}$).[33] The titration of amorphous titania in solid samples was carried out following the same method: a 10.0 mg aliquot of solid was first poured in 10.0 mL of HNO_3 (2 mol.L^{-1}) and left under stirring for 3 hours at room temperature. It has been shown elsewhere[34] that crystalline titania is not affected by such a treatment while amorphous material is totally dissolved. The Ti^{4+} concentration of the supernatant solution was then measured after centrifugation. The amount of crystalline titania in the powder was calculated from the difference between the total amount of titania and amorphous titania. The total amount of titania was measured from the weight of the inorganic residue after heating to 1000°C in TGA experiment or from total dissolution of titania in a hot $H_2SO_4/(NH_4)_2SO_4$ and subsequent spectroscopic measurement.

X-ray diffraction (XRD) measurements were performed on a Siemens D5000 diffractometer, using filtered Cu Kα radiation over 2θ range from 10^o to 80^o with a step size of 0.02° and counting time of 10 s/step. Titania powders were deposited on an amorphous glass wafer. Patterns were analysed using the DMfit software.[35] The approximate proportion of the different TiO_2 polymorphs, anatase, brookite and rutile, in the solids, were evaluated from the relative areas of the 110, 121 and 101 diffraction lines of rutile, brookite and anatase phases, respectively. The calibration parameters were taken from Magali Koelsch Ph-D work[36] and from elsewhere [28]. The size of anatase particles, D_{hkl}, was calculated applying

the Scherrer formula, $D_{hkl} = 0.9\lambda/B_{hkl}\cos\Theta$, to the line width, B_{hkl}, at half maximum corrected for the instrument broadening assuming Gaussian profile. It was assumed that line broadening is mainly due to the particle size effect. The 101, 004 and 200 diffraction lines were used once brookite lines were subtracted by fit.[28, 36] The 0.9 constant used in the Scherrer equation correspond to the calculation of spherical particles. However it was used in a good first approximation to estimate the anatase crystal dimensions in the different directions.

High resolution transmission electron micrographs (HR-TEM) were performed on a JEM-ARM 1250 at an acceleration voltage of 400.0 kV. The nanoparticles were simply ultrasonicated in ethanol and dispersed on Cu-grids (Ted Pella Inc. USA).

Thermo gravimetric analyses and differential scanning calorimetry (TGA-DSC) experiments were performed on a Jupiter STA 449C apparatus from Netzsch coupled with a GAM 200 gas analyser from In Process Instruments. Solids were heated in alumina crucibles up to 1000 °C with a heating rate of 10 °C.min^{-1} in a purified air flow.

Infrared spectra (IR) of pure amino acids and titania powders were recorded on a Nicolet Avatar 360 FT-IR apparatus. A minimum of 32 scans from 4000 to 400 cm^{-1} were collected at 2 cm^{-1} resolution versus the appropriate background spectrum.

Results and Discussion

Influence of the amino acids on the obtained titania polymorph. For pH > 1, the precipitation of titanium was immediate and complete with and without amino acid even at room temperature. For pH = 1, precipitation of most titania is observed between one and four hours at 60°C. The X-ray diffraction patterns of the powders obtained with the different amino acids at pH = 4 after one day of aging at 60°C are displayed in Figure 1 and compared to that of a reference sample (Ref) obtained without the addition of any amino acid. One first notices that every pattern displays broad diffraction lines corresponding to nanometer size particles. Amorphous titania was found in all amino acid containing samples as confirmed by UV-visible measurements. Reference sample obtained at pH = 4 is only 2% amorphous,

amino acid containing samples are at least 4% amorphous (10% with Ser, 20% with Glu and 40% with Asp). The amount of amorphous titania increased with pH up to 100% for pH = 8. The presence of amino acids in the final powder can be directly correlated with the amount of measured amorphous titania. The interaction of biological species with amorphous titania surface may inhibit, crystalline titania nucleation. The crystallization mechanism is only slowed down as full crystallization can be observed after one week of aging in the presence of amino acids. Such a delay on crystallization is already observed on the higher temperature experiments and attributed to the adsorption of amino acids on the embryos of crystalline TiO_2.[26]

In such low temperature synthesis conditions, anatase is the predominantly obtained phase.[28] In the reference sample and with all amino acids except Glu (1c), Asp (1d) and Ser (1e), a secondary phase (10 to 20% with regard to the total crystalline content) corresponding to brookite is observed at pH = 4. Brookite is replaced by rutile as a secondary phase in more acidic conditions (pH = 1) in the reference sample and with Gly, Lys and Arg. The titania phase distribution depending on the pH and the nature of the introduced amino acid is listed in Table 2.

The most interesting feature is the synthesis of pure anatase at any pH in the presence of Glu, Asp or Ser. It is also the case with His at high and low pH (1 or 6). The amino acid concentration was varied for Glu at pH = 4 and His at pH = 6 and no other crystalline phase than anatase was observed for [Ti]/[Glu] < 10 and [Ti]/[His] < 4. This means that only few amounts of amino acids are needed to control the structure of synthesized titania. The effect of the aging time on the nature of the obtained polymorph was also studied. The phase distribution between anatase and brookite polymorphs did not change significantly with time in the reference system at any pH. Similarly, pure anatase was observed even after a week of aging in the Glu system at pH = 4. On the contrary, with histidine at pH = 6, the amorphous/anatase/brookite titania mixture evolved from 60/40/0% after one day of aging to 30/65/5% after one week. Consequently, in the presence of His, amorphous titania must be converted faster into anatase than into brookite. Under kinetic control, only anatase is observed while after aging, and consequently closer to thermodynamic equilibrium, brookite is also present like in reference samples.

The control over experimental parameters such as medium acidity and reaction temperature and the use of inorganic mineralizers are the commonly used methods for titania polymorph selection.[28, 37-39] Rutile is known to be the thermodynamic polymorph[40] but it is no more the case when considering nanometer scale systems.[13] Indeed, at nanometer scale, the surface energy contribution to nanoparticles free energy can not be neglected. With a smaller average surface energy (1.3 $J.m^{-2}$) than that of rutile (1.9 $J.m^{-2}$), anatase is the most stable phase for particles smaller than 14 nm.[13] At pH = 1, the titania solubility is close to the Ti^{4+} concentration used in this study[41] and a dissolution-crystallization process can lead to the thermodynamic phase rutile. The absence of rutile at pH = 1 in Ser, Glu or Asp system may be due to the presence of [amino acids – Ti^{4+}] complexes in solution that force condensation mechanism to anatase formation as already suggested with SO_4^{2-} ions.[42, 43] Another explanation is that the release of metal ions from initially precipitated amorphous solid into solution that should lead to rutile by reprecipitation may be more difficult with the presence of amino acids at the surface of the amorphous oxide. At pH ≥ 2, the formation of brookite is also prevented using the same three amino acids Ser, Glu and Asp. Nucleation of anatase may be favored by the specific surface attachment of those amino acids that would then lower the interfacial tension of at least one of its faces. The formation of pure anatase nanoparticles has already been observed with citric acid or acetic acid as organic additives.[25, 44] At pH = 6, both His and Pro containing systems show no brookite secondary phase. As this secondary phase was recovered after longer aging time, this phase selection is only due to a kinetic effect. The attachment mode of His and Pro on titanium oxide surface at pH = 6 must be different from that of Glu, Asp and Ser.

Influence of the amino acids on titania nanoparticles size. As anatase was the most observed polymorph in the different obtained powders, the size study was focused on it. Average particle sizes were calculated from X-ray diffraction patterns using 101, 004 and 200 lines. Figure 2 shows the evolution of particle size with pH for the different introduced amino acids. Under all synthesis conditions, mean size of anatase particles was lower than 8 nm, which is significantly smaller than what

is observed through hydrothermal treatment (20-100 nm).[26] This is not surprising since higher temperature treatment usually leads to larger particles. Two different behaviors of the particles size with the pH could be observed depending on the nature of the introduced amino acids. In the presence of Gly and Pro or without amino acid (Ref) the particles size was about 6 nm at pH = 1, decreased to 5 nm at pH = 2 and then increased up to 7 nm at pH = 6. Such a size increase with pH has already been observed with a larger slope in the 2-6 pH range without any introduced amino acid.[28] The same trend was observed in the case of hydrothermal treatment in the presence of the same amino acids.[26] In the presence of the other amino acids, particles size obtained first increased from 4 nm to 8 nm (with Glu) at pH = 4 and then decreased drastically to less than 3 nm (with His) at pH = 6. A clear distinction can be made here between systems containing an amino acid without side chain functionality (Gly, Pro), whose behavior was close to the one of the reference sample, and those having a side chain functionality that may interfere in the oxide condensation process.

The influence of the [Ti]/[aa] ratio on particles size was also studied. With Glu at pH = 4 aged one day at 60°C, a maximum particle size of 9 nm was obtained for [Ti]/[Glu] = 2 while with His, a value of 6 nm was calculated for all [Ti]/[His] ratio. With His at pH = 6, the particles size increased continuously from 2 nm ([Ti]/[His] = 0.25) to 7 nm ([Ti]/[His] = 4). These experiments show that amino acids in solution have an inhibitory effect on particles growth. The increase of the aging time in all systems at pH = 4 did not have any effect on the particles size. The same trend was observed at pH = 6 with the reference sample while, in the presence of His, TiO_2 particles reached the maximum size only after four days of aging. This confirms that the equilibrium state is reached slower with His at pH = 6.

Influence of the amino acids on titania nanoparticles shape. Results on the particle shape study presented here only refer to anatase which was the major polymorph formed. The determination on the crystal shape was performed combining two techniques: X-ray diffraction and high resolution transmission electron microscopy. Three lines of the diffraction patterns were chosen for the crystal shape estimation: 101, 004 and 200 as they were shown to correspond to the more displayed faces

{101}, {001} and {100} in natural anatase crystals.[45, 46] Size measurement obtained in the reference, Glu and His samples are displayed in Figure 3.

Roughly round particles (Scheme 1a) are obtained in the reference sample except at pH = 1. For that pH value, the following size order is found: $d_{[004]} > d_{[200]} > d_{[101]}$. The corresponding reconstructed crystal shape (Scheme 1b) corresponds to an almost complete octahedron with {101} face mainly exposed. Such shapes are commonly observed in native anatase crystals.[47] The introduction of amino acids does not change particles shape except with Glu, Asp and His. As Asp and Glu samples are roughly similar, only those with Glu are presented here. The size order $d_{[004]} > d_{[200]} > d_{[101]}$ is now maintained for every pH and the calculated d_{004}/d_{101} ratio reaches a maximum value of 2.3 at pH = 4. The reconstructed model crystal shape is then an elongated octahedron (Scheme 1c) with exclusively the {101} face exposed. In the His samples, the size order is $d_{[200]} > d_{[101]} \sim d_{[004]}$ and the crystal anisotropy is most pronounced at pH = 6. The corresponding model particle shape is a platelet, with {001} face mainly exposed (see Scheme 1d).

HR-TEM micrographs displayed in Figure 4 confirmed two of the proposed shapes. Titanium oxide nanoparticles obtained at pH = 4 without amino acids form aggregates quite difficult to deagglomerate (Figure 4a). The observation of fringes in the aggregate indicates that most of the solid is made of nanocrystalline anatase as the distance between fringes correspond to that between (101) anatase planes. Nanoparticles can be described as spheroids in the 5-10 nm size range. TiO_2 nanoparticles formed in the presence of glutamic acid seem less aggregated (Figure 4b). They also display fringes corresponding to (101) anatase planes but here two sets of fringes making a cross angle of ca 130° can be observed. Using those fringes we were able to deduce that crystals are developed preferentially in the [001] direction as indicated by the arrow. Moreover, particles are not straight rods but are faceted by {101} face, as shown by the dashed lines. These results are in good agreement with XRD calculations but when comparing to model crystal shape one must state that the d_{004}/d_{101} ratio can exceed in some cases the 2.4 limit value corresponding to elongated octahedrons. Micrographs obtained in the His system only show small crystalline domains among high amounts of amorphous titania and particles shape can not be analyzed.

TiO_2 nanoparticles obtained through hydrothermal treatment in the presence of amino acids display a similar behavior.[26] Indeed, at pH = 10.5, nanoparticles elongated in the [001] direction are observed exclusively in the Glu and Asp containing systems. Ellipsoidal particles are obtained in the 9-11 pH range while ill-defined spheroids are obtained in the 2-6 pH range. The same driving force probably controls the particles shape in the two studies and the difference in the pH range on which this control is effective may be due to the pH range shrinkage with hydrothermal conditions.

In order to address in detail the shape control, one must consider that, under thermodynamic control, particles morphology is driven by the reduction of surface energy. Particle growth is controlled by the minimization of the surface area that corresponds to the highest surface energy. Indeed, the total surface energy defined as $\Sigma_i(\gamma_i A_i)$ with A_i the size of exposed surface i and γ_i its interfacial tension, is minimized to reach the equilibrium state. For more detailed thermodynamic explanations, a modeling of oxide nanoparticles size and shape tailoring was proposed by Jolivet *et al*.[48] The relation between the modification of experimental conditions and the nanoparticles shape may be found in the change in the different faces interfacial tension. The variation of this parameter is given by Gibb's law, $d\gamma = -\Sigma\Gamma_i d\mu_i$ with Γ_i the density of adsorption of species i of electrochemical potential μ_i.[49] By modifying the pH of the reaction, the adsorption of protons on the oxide surface is changed. The chemical structure of {101} and {001} faces are different, so their protonation state with pH are also different and can be estimated using oxide surface simulation software such as MUSIC.[50-52] Using a qualitative approach, we can state that the {001} face display a higher density of protonation sites and then its maximum charge must be higher than the one of the {101} face. The interfacial tension variation with pH is related to the maximum charge of the oxide surface by a complex relation[48] and it is more pronounced with higher surface charge. The less charged surface {101} must then be more present at low pH (far from the point of zero charge). The preferential growth of anatase particles in the [001] direction at lower pH is in good agreement with that statement. Such a trend was also observed in hydrothermal coarsening of anatase nanoparticles.[15]

The interfacial tension balance between the different faces is also altered by selective adsorption of amino acids on a specific oxide surface. Thus, Glu and Asp may interact more strongly with the {101} face of anatase than with the {001} face as proposed in Figure 5. That way, the {101} face displays a lower interfacial tension and is consequently more stabilized. In other words, the {101} face must be covered by the preferential complexation of amino acids leading to a preferential growth in the [001] direction and the total disappearance of the competitive {001} face.

The particle shape evolution with [Ti]/[Glu] ratio at pH = 4 is shown in Figure 6. Particles size first increases equally in every direction with increasing [Ti]/[Glu] ratio. A nearly constant value of d_{004}/d_{101} = 2.4 was calculated up to [Ti]/[Glu] = 2. The aspect ratio then decreases with the amount of glutamic acid in solution. The same trend and the same threshold value [Ti]/[aa] = 2 is observed in the hydrothermal system with a maximum aspect ratio of 4.[26] The threshold value [Ti]/[aa] = 2 is also valid in this study with His at pH = 6. At low [Ti]/[His] values, size in the [200] direction is significantly greater than in the other two the directions while at high [Ti]/[His] values all the directions are equivalent in size. Another interesting feature is that, at a fixed [Ti]/[Glu] = 1/2 ratio, a longer aging time did not change particles shape in the Glu system at pH = 4 whereas anisotropy was lost after four days of aging in the His system at pH = 6.

This value of [Ti]/[Glu] = 2 confirms that the presence of a Glu layer on the surface of the oxide particle is responsible for the shape control. Assuming that, for that specific value of [Ti]/[Glu] ratio all introduced amino acids are present on the {101} surface of all anatase nanoparticles, the Glu surface coverage density is 0.3 nm^{-2}. Each of the three possible interacting hydroxyl surface groups μ-OH presents a site density on the {101} face of 5.2 nm^{-2} as calculated from the crystallographic structure. Moreover, assuming full monolayer coverage of the oxide surface by Glu assimilated to a 0.8*0.4 nm rectangle lying parallel to the surface, the minimum Glu density calculated is 3 nm^{-2}. So the full coverage of the surface is not reached at the threshold value but is enough to stabilize the formation of a complete {101} faceted octahedron. The stabilization of the {101} face with Glu is preserved over time

while the stabilization of the {001} face is partially lost with His after seven days so we can say that the binding of amino acid to the surface is stronger in the first system.

Other examples of organic species used as shape controller are present in the literature.[18, 22, 23, 25, 42, 53] The use of tetramethylammonium ions (TMA^+), triethanolamine, acetyl acetonate or acetic acid as additives in hydrothermal crystallization of titania also lead to the formation of elongated particles along the [001] direction. The saw tooth shape of those particles with the {101} face exposed clearly shows that this surface is specifically stabilized. But none of these studies gave a clear explanation of that shape control property.

Presence of the amino acids on titania nanoparticles surface. The explanations discussed above for titania structure, size and shape controlled by amino acids are based on the assumption that interactions between organic and inorganic components occur during synthesis. These interactions may happen in aqueous solution, at the amorphous oxide interface or at the crystalline oxide interface. In the last two cases, amino acids must still be present in the final product. That is why the presence of organic species has been checked.

The presence of organic material was first estimated by infrared spectra of the powders. Titanium oxide network produces vibration bands at wavenumbers lower than 1000 cm^{-1} and the hydroxyl surface groups contribute to a broad band at ca. 1600 cm^{-1}. Vibration bands in the 1200-1600 cm^{-1} range may be attributed to amino acids. Except in the Glu, Asp and Ser systems, very few organic species can be observed in the powders obtained at a pH $\leq$ 4. The washing and ultrasonication treatments have removed quite efficiently organic materials which were not bound to the oxide surface. The relative amount of organic species is much more important in the Glu and Asp systems than in the Ser one. At pH = 6, all infrared spectra present vibration bands corresponding to the amino acids. In summary, amino acids adsorption on the oxide surface depends on its chemical composition and on solution pH. The adsorption of amino acids on titanium oxide has already been studied as first step for biological adhesion on titanium implants studies[54-58] or for their photocatalysis mineralization.[59-61] Different

techniques such as supernatant analysis,[62] thermal desorption spectroscopy (TDS),[63, 64] attenuated total reflectance infrared spectroscopy (ATR-IR)[55, 56, 58] and X-ray photoelectron spectroscopy (XPS)[65-68] have been used to determine the adsorption mode.

Electrostatic interactions are proposed in many studies. The sign of oxide surface charge changes at the point of zero charge (PZC). This PZC is 4.6 for amorphous titania[34] and is between 5.4 and 6.0 for crystalline polymorphs.[69] As for amino acids, charge depends directly on the acid base properties of the chemical groups of their main and side chains. pKa values of the different amino acids are listed in Table 1. In the first experimental study of amino acids adsorption of titania, Glu is adsorbed on titania in the 3-4 pH range and Lys, in the 6-10 pH range.[62] These results are explained by attractive electrostatic interactions. The presence of positively charged amino acids on particles synthesized at pH = 6 in our study may also be explained by such interactions as titania surface is slightly negatively charged. Adsorption of Glu and Asp at pH = 4 can also be explained that way.

However, the adsorption of Glu, Asp and Ser at any pH can not be explained only by electrostatic considerations. Indeed, with isoelectric point values of 3.22 and 2.77 respectively, Glu and Asp should only adsorb to the oxide surface in the 3-5 pH range. Amino acids such as Gly and Ser are in a zwitterionic form at pH = 6 and are still present in small amounts at oxide surface. Other studies have also evidenced the adsorption of Ser, Met, Glu and Asp in the 2-6 pH range even if the first two are positively or not charged.[67, 68] Moreover, an increase of solution ionic strength did not affect Asp adsorption on TiO_2 particles, what rules out a purely electrostatic interaction.[55]

The infrared spectrum of the titania powder obtained in the presence of Glu at pH = 4 was studied more accurately and compared with data displayed in the literature (Table 3). The measured values are in good agreement with those obtained by ATR-IR study of glutamic acid adsorption on a TiO_2 surface.[58] No ν_S(COOH) could be observed around 1713 cm^{-1} in our sample indicating that the side chain carboxylic group is deprotonated upon adsorption to TiO_2. The two $\nu_{AS}(COO^-)$ bands were observed at slightly lower wavenumber values than elsewhere [58] but this may be due to the nature of the oxide surface[70] or to a difference of the system pH = 4 here instead of 2.9 in ref. [58]. The positions of

those two bands are consistent with a bidentate coordination mode of the carboxylate group to two titanium (as proposed in Figure 5) or a chelation to the same surface titanium.[71] In any case, the two carboxylate groups seem to be involved in the adsorption of the amino acid on the oxide surface. The 1446 cm^{-1} band corresponds to the bending of the side chain CH_2. The observed difference with measured value in solution can be explained by the binding of both ends of the chain on the oxide surface. The last interesting band at 1405 cm^{-1} corresponds to the $\nu_S(COO^-)$ and seems unaffected by the adsorption on titania. These data show that adsorption of amino acids containing two carboxylate groups on the titanium oxide surface is due to the chelation of both groups to surface titanium ions.

Results presented here are in fair agreement with already published ATR-IR and XPS data on amino acids adsorption on titania surfaces. Both techniques showed that the carboxylate group is interacting with the oxide surface[58, 67, 68] and only one study on Asp proposed $-NH_2$ as the main interacting group.[55] Different described structures for amino acids adsorption on TiO_2 are given in Scheme 2. The first structure corresponding to interactions through hydrogen bonds was proposed from simulations of cysteine adsorption on rutile.[72] An unionized molecule is presented in that structure as calculations were performed in vacuum where this form is more stable than the zwitterionic form. The other three structures correspond to an inner sphere complexation of amino acids to surface Ti^{4+} ions with different coordination modes of the carboxylate groups proposed in the literature.[70, 71, 73-75] With dicarboxylate amino acids Asp and Glu, binding through more than one group was proposed.[55, 58] In structure 3, a $-NH_2$ group is proposed as another ligand in the coordination sphere of a second Ti^{4+} surface ion.[55] In structure 4, Glu forms a surface chelate complex via both carboxylate groups.[58] The presence of both carboxylates groups in the inner sphere of surface titanium ions evidenced in the present study is in good agreement with the structure 4. Consequently, this structure is the most probable for Glu and Asp adsorption.

More accurate information about the amount of organic species in the powders can be obtained from TGA-DSC coupled with a gas analyzer in order to discriminate weight loss due to adsorbed water from that of organic species. The powder obtained with Glu at pH = 4 contains 4%.wt of water and 15%.wt of

organic material (Figure 7). This organic material is released in two steps: the first and most important desorption step starts at 280°C with a maximum rate around 300°C and the second step starts at 400°C with a maximum at 420°C. Almost no weight loss is observed above 500°C. The powder obtained in the presence of glycine contains roughly the same amount of entrapped water as the former sample but only 5%.wt of organic species. This organic material is desorbed in three steps with maximum rate at 120, 280 and 450°C. This is in good agreement with literature data.[63] Low temperature desorption corresponds to a weekly bound state while higher temperature release corresponds to the thermal decomposition of glycine into smaller sub-units. With glutamic acid, no low temperature desorption was observed indicating a stronger interaction with oxide surface and most of organic material was released as carbon dioxide. This is in good agreement with the complexation of two carboxylate groups with glutamic acid instead of only one with glycine.

A last possibility of amino acid-Ti(IV) interaction that may impact on the condensation of an oxide phase is the formation of a bio-inorganic complex in solution. Indeed, the formation of a Ti(IV)-acetoacetate complex from alkoxide solution changes drastically the reactivity of the inorganic precursor.[21] The complexation of amino acids to Ti^{4+} has already been reported but two cyclopentadienyl ligands are also needed in the coordination sphere.[76-79] The amino acid binds to the metallic center only through the carboxylate group as a two electrons donor ligand and the formed complex in organic solvent is rapidly dissociated in aqueous solution.[76] So the formation of a Ti(IV)-aa complex as driving force for nanoparticle modification can not be completely ruled out but the surface interaction modes must be preferentially taken into account.

Conclusion and outlook

Amino acids have been used for the first time as controlling agent in the sol-gel formation of titanium oxide bellow 100°C. Different parameters such as pH, aging time, amino acid nature and concentration have been studied. The presence of the amino acids has an impact on the kinetic and thermodynamic of the crystalline oxide formation. More specifically, the crystallization is slower with glutamic acid. Its

presence leads exclusively to the formation of the anatase structure with an elongated octahedron shape. This was explained by the proposition of a specific stabilization of the {101} face of anatase by complexation of both carboxylate group of the amino acid on that surface.

Experimental results and data taken from the literature demonstrate that amino acids can be present on both amorphous and crystalline titania particles. ATR-IR studies on dicarboxylate adsorption on different titania polymorphs have shown that one to three different complexes could be observed on each structure.[70] This means that the dicarboxylate complexation strength depends also on the geometry of the oxide surface.

The question that must now be answered is why the amino acid Glu binds preferentially to the {101} surface of anatase and His to the {001} one. A possible answer is that an epitaxial relation exists between the metallic sites of the chosen surface and the corresponding amino acid. A molecular dynamic simulation of Glu and His approach and adsorption to different anatase surfaces is mandatory to answer that question in full.

The selection of a polymorph and a specifically exposed face are of particular interest in applications of photocatalysis and solar cells. These new results should motivate further investigations on titania bio-controlled syntheses in aqueous solution.

Acknowledgment: The authors are indebted to Dr. Phillipp for the acquisition of TEM images and Gerhard Kaiser for performing thermo gravimetric experiments. They thank the Dr. Diawara for providing the software ModelView used in Figure 5. They also thank the Alexander von Humboldt foundation for the post-doctoral grant for Olivier Durupthy.

Supporting Information Available

No additional supporting information. This information is available free of charge via the Internet at http://pubs.acs.org

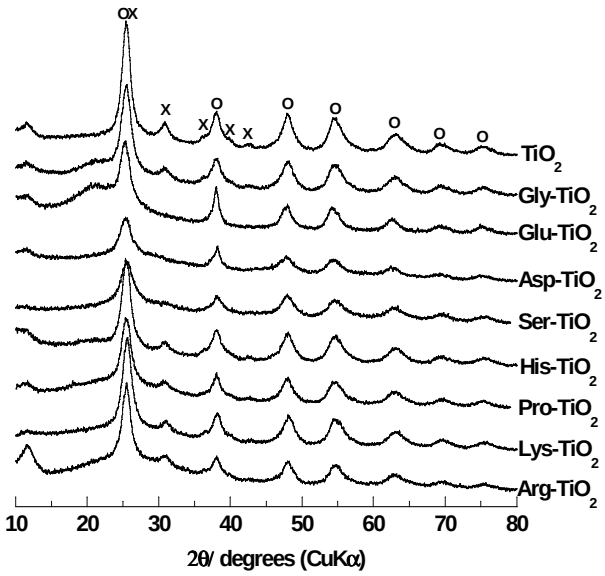

Figure 1. X-ray diffraction patterns of titania powders obtained at pH = 4 after 1 day aging at 60°C without or with various amino acids. Lines marked with a circle correspond to anatase and with a cross to brookite.

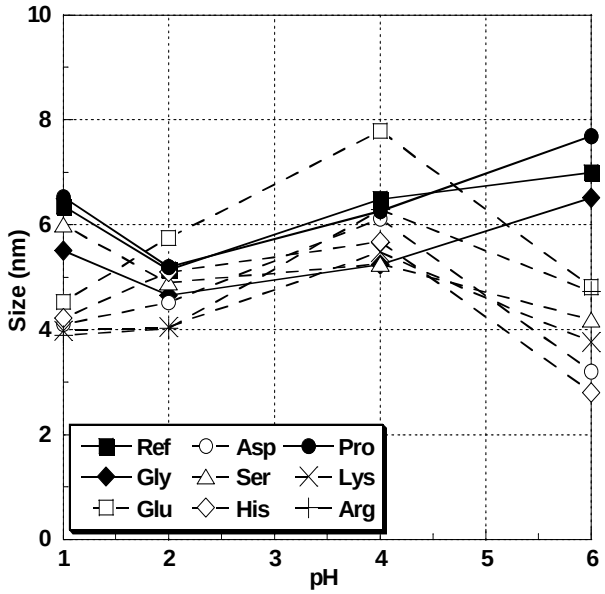

Figure 2. Mean size of anatase nanoparticles calculated using the Scherrer equation as a function of the pH of the starting solution and the nature of the introduced amino acid. Error bars are not presented on the graph but generally correspond to ± 0.5 nm.

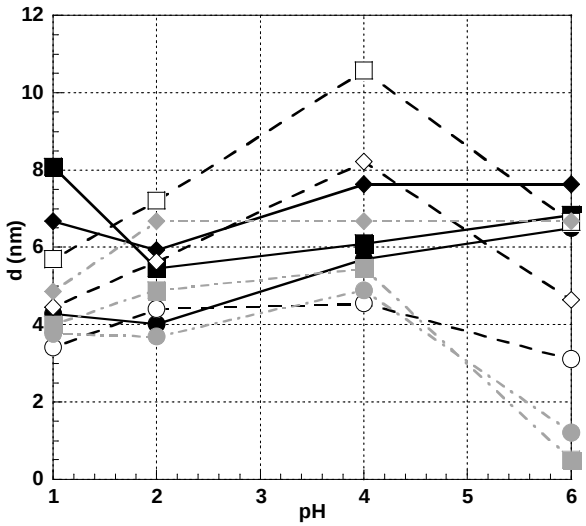

Figure 3. Mean size d of anatase nanoparticles in different crystallographic directions calculated using the Scherrer equation as a function of the pH of the starting solution and the nature of the introduced amino acid. Black dots correspond to Ref samples, white ones to Glu samples and grey ones to His samples. Circles correspond to measurements in the [101] direction, squares to measurements in the [004] direction and rhombuses to measurements in the [200] direction. Error bars are not presented on the graph but generally correspond to ± 1 nm.

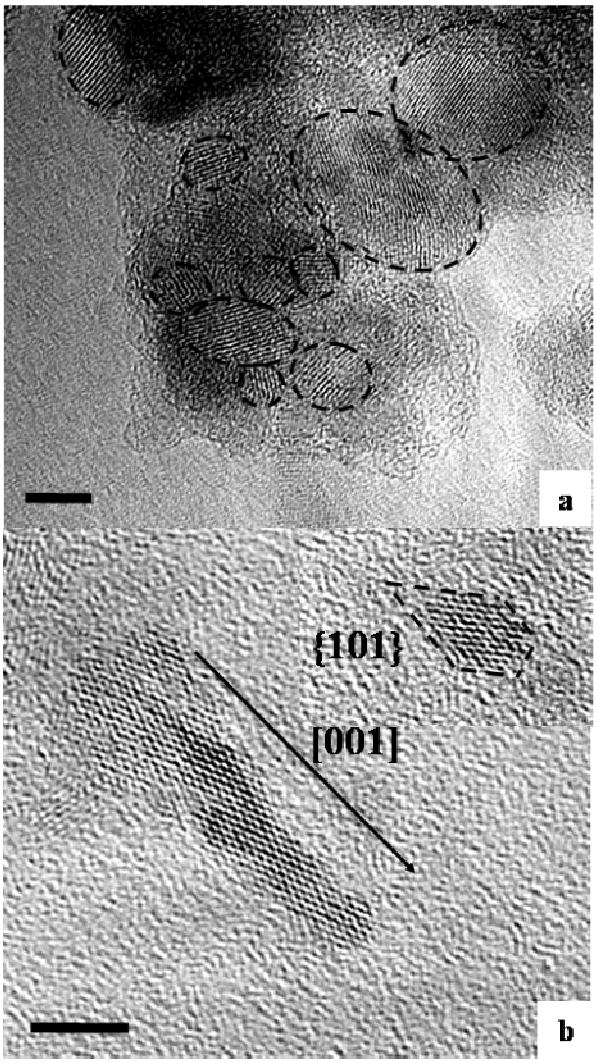

Figure 4. High resolution electron micrographs of titania nanoparticles obtained at pH = 4 after one day of aging, (a) without and (b) with glutamic acid in the reacting medium. Scale bars correspond to 5 nm.

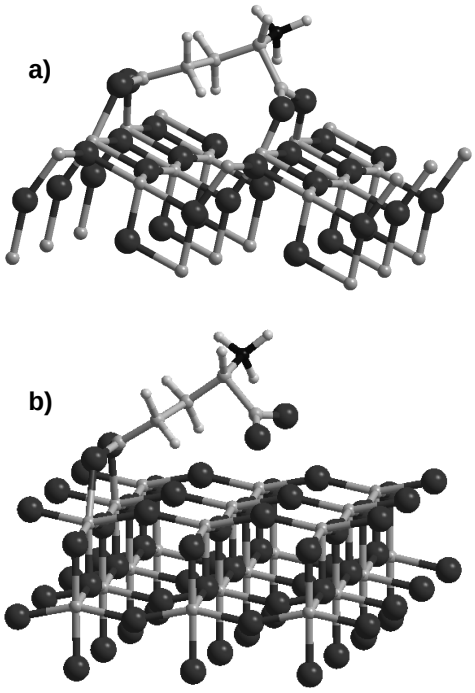

Figure 5. Possible model of glutamic acid adsorption on the a) {101} face and b) {001} face of the anatase polymorph. For clarity purpose, surface hydroxyl groups are not represented on the oxide surfaces.[80]

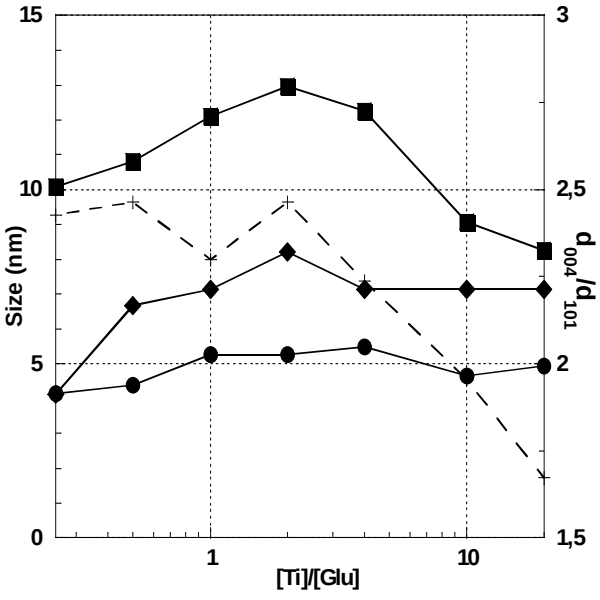

Figure 6. Evolution of anatase particles shape with [Ti]/[Glu] ratio. Circles correspond to measurements in the [101] direction, squares to measurements in the [004] direction and diamonds to measurements in the [200] direction. Crosses and dashed line represent the d_{004}/d_{101} ratio.

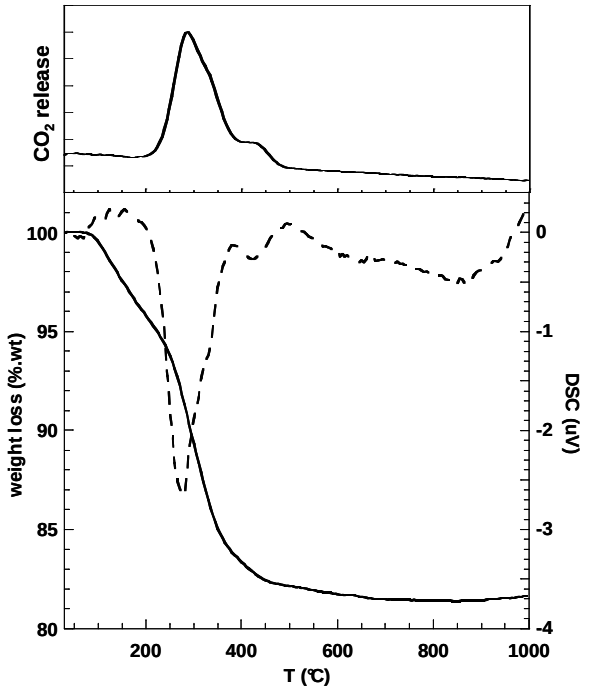

Figure 7. Thermogravimetric (solid) and differential scanning calorimetry (dashed) curves of the titania powder obtained at pH = 4 after 1 day in the presence of Glu. On top, the relative amount of released CO_2 gas as a function of temperature is represented.

Scheme 1. Atoms drawing of model anatase crystals rebuild from Debye Scherrer measurements of crystal size. The upper and lower surfaces correspond to the {001} plane and the side surfaces to {101} planes. The calculated model systems are a) Ref pH = 4, b) Ref pH = 1, c) Glu pH = 4 and d) His pH = 6.

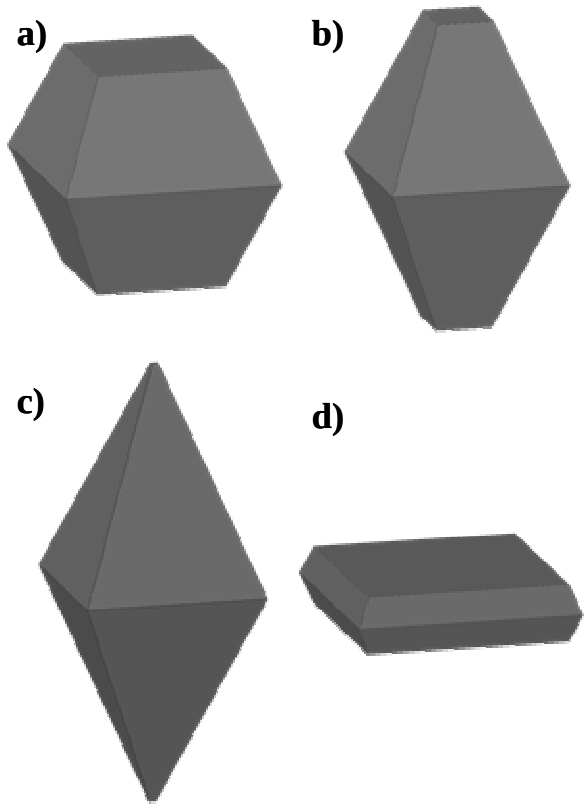

Scheme 2. Possible structures for amino acids adsorbed on the TiO_2 surface.[55, 58, 72]

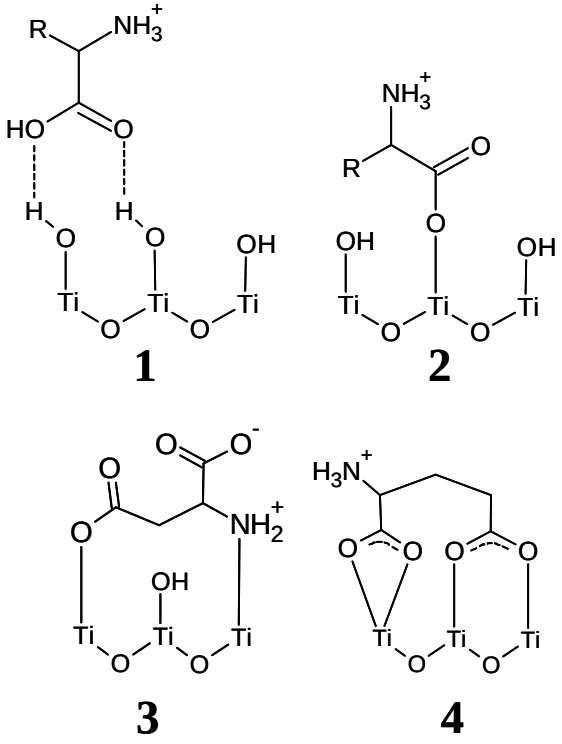

Amino acid	*Molecular structure*	*pKa*	*IEP*
Glycine (Gly)	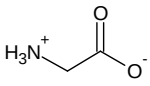	2.35, 9.78	5.97
Glutamic acid (Glu)	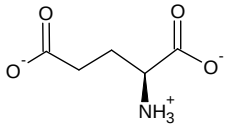	2.10, **4.07**, 9.47	3.22
Aspartic acid (Asp)	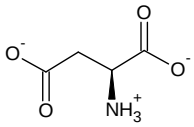	2.10, **3.86**, 9.82	2.77
Serine (Ser)	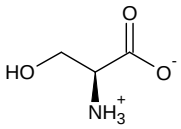	2.21, 9.15	5.68
Histidine (His)	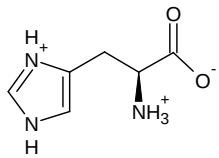	1.77, **6.10**, 9.18	7.47
Proline (Pro)	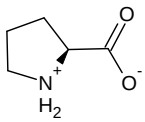	2.00, 10.60	6.30
Lysine (Lys)	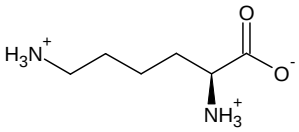	2.18, 8.95, **10.53**	9.59
Arginine (Arg)	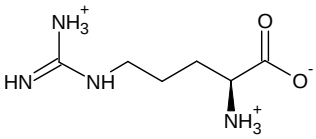	2.01, 9.04, **12.48**	11.15

Table 1. Molecular structure of the different amino acids used. pKa and isoelectric point values of the acid-base groups present on the amino acids (bold values correspond to side chain group).

amino acid	pH = 1	pH = 2	pH = 4	pH = 6	pH = 8
-	A + R	A + b	A + b	A + b	amorphous
Gly	A + r	A + b	A + b	A + b	amorphous
Glu	A	A	A	A	amorphous
Asp	A	A	A	A	amorphous
Ser	A	A	A	A	amorphous
His	A	A + b	A + b	A	amorphous
Pro	A + b	A + b	A + b	A	amorphous
Lys	A + R	A + b	A + b	A + b	amorphous
Arg	A + R	A + b	A + b	A + b	amorphous

Table 2. Titania polymorphs distribution as a function of the pH of the reacting solution and the nature of the introduced amino acid. A stand for anatase, b stands for brookite and R or r stand for rutile. Capital letters correspond to the predominant polymorph and small letters to the secondary phase.

Sample	$\nu_S(COOH)$	$\nu_{AS}(COO^-)$	$\nu_{AS}(COO^-)$	$\delta(CH_2)$	$\nu_S(COO^-)$
In solution [58]	1713	1613	1540	1456	1405
Adsorbed [58]	/	1600	1537	1449	1405
This study	/	1590	1530	1446	1405

Table 3. Infrared spectroscopic data of glutamic acid carboxylate groups in solution at pH = 3.2 according to ref. [58], adsorbed on a TiO_2 film at pH = 2,9 according to ref. [58] and in the present system at pH = 4.0. All vibration band values are expressed in cm^{-1}.

References

(1) Reisch, M. *Chem. Eng.* **2001,** *79*, 23-30.
(2) Sakai, A. *Fragrance Journal* **2003,** *31*, 81.
(3) Fujishima, A.; Honda, K. *Nature* **1972,** *238*, 37.
(4) Hoffmann, M. R.; Martin, S. T.; Choi, W.; Bahnemann, D. W. *Chem. Rev.* **1995,** *95*, 69-96.
(5) Vinodgopal, K.; Hotchandani, S.; Kamat, P. V. *J. Phys. Chem.* **1993,** *97*, 9040-9044.
(6) Bonhôte, P.; Gogniat, E.; Campus, F.; Walder, L.; Gratzel, M. *Displays* **1999,** *20*, 137-144.
(7) Bonhôte, P.; Moser, J.-E.; Humphry-Baker, R.; Vlachopoulos, N.; Zakeeruddin, S. M.; Walder, L.; Grätzel, M. *J. Am. Chem. Soc.* **1999,** *121*, 1324 - 1336.
(8) Lin, H.-M.; Keng, C.-H.; Tung, C.-Y. *Nanostruct. Mater.* **1997,** *9*, 747-750.
(9) Ferroni, M.; Guidi, V.; Martinelli, G.; Faglia, G.; Nelli, P.; Sberveglieri, G. *Nanostruct. Mater.* **1996,** *7*, 709-718.
(10) Croce, F.; Appetecchi, G. B.; Persi, L.; Scrosati, B. *Nature* **1998,** *394*, 456-458.
(11) Kalyanasundaram, K.; Gratzel, M. *Coord. Chem. Rev.* **1998,** *177*, 347-414.
(12) Barbé, C. J.; Arendse, F.; Comte, P.; Jirousek, M.; Lenzmann, F.; Shklover, V.; Grätzel, M. *J. Am. Ceram. Soc.* **1997,** *80*, 3157-3171.
(13) Zhang, H.; Banfield, J. F. *J. Mater. Chem.* **1998,** *8*, 2073-2076.
(14) Aruna, S. T.; Tirosh, S.; Zaban, A. *J. Mater. Chem.* **2000,** *10*, 2388-2391.
(15) Penn, R. L.; Banfield, J. F. *Geochim. Cosmochim. Acta* **1999,** *63*, 1549-1557.
(16) Wang, C.-C.; Ying, J. Y. *Chem. Mater.* **1999,** *11*, 3113-3120.
(17) Uekawa, N.; Kajiwara, J.; Kakegawa, K.; Sasaki, Y. *J. Colloid Interface Sci.* **2002,** *250*, 285-290.
(18) Gao, Y.; Elder, S. A. *Mater. Lett.* **2000,** *44*, 228-232.
(19) Zaban, A.; Aruna, S. T.; Tirosh, S.; Gregg, B. A.; Mastai, Y. *J. Phys. Chem. B* **2000,** *104*, 4130-4133.
(20) Matijevic, E. *Acc. Chem. Res.* **1981,** *14*, 22-29.
(21) Scolan, E.; Sanchez, C. *Chem. Mater.* **1998,** *10*, 3217-3223.
(22) Chemseddine, A.; Moritz, T. *Eur. J. Inorg. Chem.* **1999,** *1999*, 235-245.
(23) Sugimoto, T.; Zhou, X.; Muramatsu, A. *J. Colloid Interface Sci.* **2003,** *259*, 43-52.
(24) Sugimoto, T.; Zhou, X.; Muramatsu, A. *J. Colloid Interface Sci.* **2003,** *259*, 53-61.
(25) Zhu, Y. C.; Ding, C. X. *Nanostruct. Mater.* **1999,** *11*, 427-431.
(26) Kanie, K.; Sugimoto, T. *Chem. Commun.* **2004,** *2004*, 1584-1586.
(27) Pottier, A.; Chanéac, C.; Tronc, E.; Mazerolles, L.; Jolivet, J.-P. *J. Mater. Chem.* **2001,** *11*, 1116-1121.
(28) Pottier, A.; Cassaignon, S.; Chanéac, C.; Villain, F.; Tronc, E.; Jolivet, J.-P. *J. Mater. Chem.* **2003,** *13*, 877-882.
(29) Mann, S.; Webb, J.; Williams, R. J. P., *Biomineralization: chemical and biochemical perspectives*. ed.; Wiley-VCH: New York, 1989; p 539.
(30) Bazylinski, D. A.; Frankel, R. B.; Heywood, B. R.; Mann, S.; King, J. W.; Donaghay, P. L.; Hanson, A. K. *Appl. Environ. Microbiol.* **1995,** *61*, 3232-3239.
(31) Weiner, S.; Traub, W.; Parker, S. B. *Philos. Trans. R. Soc. London, Ser. B* **1984,** *304*, 425-434.
(32) Constantz, B. R. *Palaios* **1986,** *1*, 152-157.
(33) Charlot, G., *Les méthodes de la chimie analytique : analyse quantitative minérale*. 4 ed.; Masson: Paris, 1961; p 1024.

(34) Sugimoto, T.; Zhou, X. *J. Colloid Interface Sci.* **2002,** *252*, 347-353.
(35) Massiot, D.; Fayon, F.; Capron, M.; King, I.; Le Calvé, S.; Alonso, B.; Durand, J.-O.; Bujoli, B.; Gan, Z.; Hoatson, G. *Magn. Reson. Chem.* **2002,** *40*, 70-76.
(36) Koelsch, M. Nanoparticules de TiO2 : contrôle structural, morphologique, dimensionnel et propriétés électrochimiques. Université P. et M. Curie, Paris, 2004.
(37) Boiadjieva, T.; Cappelletti, G.; Ardizzone, S.; Rondinini, S.; Vertova, A. *Phys. Chem. Chem. Phys.* **2004,** *6*, 3535-3539.
(38) Lee, G. H.; Zuo, J.-M. *J. Am. Ceram. Soc.* **2004,** *87*, 473-479.
(39) Hu, Y.; Tsai, H.-L.; Huang, C.-L. *Mater. Sci. Eng. :A* **2003,** *344*, 209-214.
(40) Mitsuhashi, T.; Kleppa, O. J. *J. Am. Ceram. Soc.* **1979,** *62*, 356-357.
(41) Baes, C. F.; Mesmer, R. E., *Hydrolysis of cations*. ed.; Wiley: New York, 1976.
(42) Li, Y.; Lee, N.-H.; Hwang, D.-S.; Song, J. S.; Lee, E. G.; Kim, S.-J. *Langmuir* **2004,** *20*, 10838-10844.
(43) Zhang, Q.; Gao, L.; Guo, J. *J. Eur. Ceram. Soc.* **2000,** *20*, 2153-2158.
(44) Yin, H.; Wada, Y.; Kitamura, T.; Sumida, T.; Hasegawa, Y.; Yanagida, S. *J. Mater. Chem.* **2002,** *12*, 378-383.
(45) Hebenstreit, W.; Ruzycki, N.; Herman, G. S.; Gao, Y.; Diebold, U. *Phys. Rev. B* **2000,** *62*, R16334-R16336.
(46) Diebold, U. *Surf. Sci. Rep.* **2003,** *48*, 53-229.
(47) Oliver, P. M.; Watson, G. W.; Kelsey, E. T.; Parker, S. C. *J. Mater. Chem.* **1997,** *7*, 563-568.
(48) Jolivet, J.-P.; Froidefond, C.; Pottier, A.; Chanéac, C.; Cassaignon, S.; Tronc, E.; Patrick Euzen *J. Mater. Chem.* **2004,** *14*, 3281-3288.
(49) Stol, R. J.; DeBruyn, P. L. *J. Colloid Interface Sci.* **1980,** *75*, 185-198.
(50) Hiemstra, T.; De Wit, J. C. M.; Van Riemsdijk, W. H. *J. Colloid Interf. Sci.* **1989,** *133*, 105-117.
(51) Hiemstra, T.; Van Riemsdijk, W. H.; Bolt, G. H. *J. Colloid Interface Sci.* **1989,** *133*, 91-104.
(52) Hiemstra, T.; Venema, P.; Riemsdijk, W. H. V. *J. Colloid Interface Sci.* **1996,** *184*, 680-692.
(53) Chu, R.; Yan, J.; Lian, S.; Wang, Y.; Yan, F.; Chen, D. *Solid State Commun.* **2004,** *130*, 789-792.
(54) Giacomelli, C. E.; Avena, M. J.; De Pauli, C. P. *J. Colloid Interf. Sci.* **1997,** *188*, 387-395.
(55) Giacomelli, C. E.; Avena, M. J.; De Pauli, C. P. *Langmuir* **1995,** *11*, 3483-3490.
(56) Roddick-Lanzilotta, A. D.; Connor, P. A.; McQuillan, A. J. *Langmuir* **1998,** *14*, 6479-6484.
(57) Roddick-Lanzilotta, A. D.; McQuillan, A. J. *J. Colloid Interface Sci.* **1999,** *217*, 194-202.
(58) Roddick-Lanzilotta, A. D.; McQuillan, A. J. *J. Colloid Interface Sci.* **2000,** *227*, 48-54.
(59) Hidaka, H.; Ajisaka, K.; Horikoshi, S.; Oyama, T.; Zhao, J.; Serpone, N. *Catal. Lett.* **1999,** *60*, 95-98.
(60) Hidaka, H.; Horikoshi, S.; Ajisaka, K.; Zhao, J.; Serpone, N. *J. Photochem. Photobiol., A* **1997,** *108*, 197-205.
(61) Horikoshi, S.; Serpone, N.; Zhao, J.; Hidaka, H. *J. Photochem. Photobiol., A* **1998,** *118*, 123-129.
(62) Tentorio, A.; Canova, L. *Colloids Surf.* **1989,** *39*, 311-319.
(63) Lausmaa, J.; P. Löfgren, B. K. *J. Biomed. Mater. Res.* **1999,** *44*, 227-242.
(64) Fleming, G. J.; Idriss, H. *Langmuir* **2004,** *20*, 7540-7546.
(65) Soria, E.; Colera, I.; Roman, E.; Williams, E. M.; de Segovia, J. L. *Surf. Sci.* **2000,** *451*, 188-196.
(66) Soria, E.; Roman, E.; Williams, E. M.; de Segovia, J. L. *Surf. Sci.* **1999,** *433-435*, 543-548.
(67) Schmidt, M. *Arch. Orthop. Trauma Surg.* **2001,** *121*, 403-410.
(68) Schmidt, M.; Steinmann, S. G. *Fresenius J. Anal. Chem.* **1991,** *341*, 412-415.
(69) Kosmulski, M. *Adv. Colloid Interface Sci.* **2002,** *99*, 255-264.
(70) Hug, S. J.; Bahnemann, D. *J. Electron. Spectrosc. Relat. Phenom.* **2006,** *150*, 208-219.
(71) Rotzinger, F. P.; Kesselman-Truttmann, J. M.; Hug, S. J.; Shklover, V.; Grätzel, M. *J. Phys. Chem. B* **2004,** *108*, 5004-50017.
(72) Langel, W.; Menken, L. *Surf. Sci.* **2003,** *538*, 1-9.

(73) Wilson, J. N.; Idriss, H. *Langmuir* **2005,** *21*, 8263-8269.
(74) Weisz, A. D.; Garcia Rodenas, L.; Morando, P. J.; Regazzoni, A. E.; Blesa, M. A. *Catal. Today* **2002,** *76*, 103-112.
(75) Vittadini, A.; Selloni, A.; Rotzinger, F. P.; Grätzel, M. *J. Phys. Chem. B* **2000,** *104*, 1300-1306.
(76) Pérez, Y.; López, V.; Rivera-Rivera, L.; Cardona, A.; Meléndez, E. *J. Biol. Inorg. Chem.* **2005,** *10*, 94-104.
(77) Bína, R.; Císarová, I.; Pavlista, M.; Pavlík, I. *Appl. Organomet. Chem.* **2004,** *18*, 262-263.
(78) Klapoetke, T. M.; Koepf, H.; Tornieporth-Oetting, I. C.; White, P. S. *Organometallics* **1994,** *13*, 3628-3633.
(79) Tornieporth-Oetting, I. C.; White, P. S. *Organometallics* **1995,** *14*, 1632-1636.
(80) Diawara, B. *ModelView*, Paris, 2007.

For Table of Contents Use Only

Bio-inspired synthesis of crystalline TiO_2: Effect of amino acids on nanoparticles structure and shape.

Olivier Durupthy*, Joachim Bill, and Fritz Aldinger

The use of amino acids as additives to the thermohydrolysis of titanium tetrachloride solutions is an innovative bio-inspired process for the synthesis of titania. With certain amino acids such as glutamic acid, pure anatase nanoparticles were obtained displaying an elongated shape. Bio-control is performed through the modification of the oxide/solution interface.